Microelectronic Engineering 125 (2014) 73–77

Contents lists available at ScienceDirect

Microelectronic Engineering

journal homepage: www.elsevier.com/locate/mee

An analytical model for calculating the pull-in voltage of micro cantilever beams subjected to tilted and curled effects

Yuan-Te Huang, He-Ling Chen, Wensyang Hsu *

Department of Mechanical Engineering, National Chiao Tung University, 1001 Ta Hsueh Road, Hsinchu, Taiwan

ARTICLE INFO

Article history:
Available online 7 January 2014

Part of content in this paper has been presented in 39th International Conference on Micro and Nano Engineering, 16-19 Sep. 2013, at London.

Keywords:
Cantilever beam
Curled deformation
Tilted deformation
Pull-in voltage
Deformation function

ABSTRACT

Pull-in is a fundamental phenomenon in electrostatic micro devices. In previous studies on modeling the pull-in voltage of suspended micro cantilever beam subject to residual stress, only curled deformation was considered. This study proposed a modified deformation function, which considered both curled and tilted deformations caused by gradient stress and mean stress, to calculate the pull-in voltage of the suspended cantilever beam with residual deformations.

In order to verify the proposed analytical model, suspended poly-silicon cantilever beams with three different lengths, 260 μm, 295 μm and 330 μm, are fabricated through surface micromachining process. It is shown that the residual deformations include both curled and tilted deformations, where the tilted angle and radius of curvature can be identified by white light interferometer (WLI). By comparing the analytical results with measurement results on pull-in voltages, it is found that while only considering curled effect, the average error of calculated pull-in voltage is 10.5%. On the other hand, when both tilted and curled effects are considered, the average error is reduced to 3.2%, which verifies the accuracy improvement of the proposed analytical model.

1. Introduction

Electrostatically actuated micro cantilever beams are widely used in Micro Electro Mechanical Systems (MEMS), such as micro-sensors [1,2], microactuators [3,4], and AFM structures [5]. For electrostatic transducers, pull-in is a basic phenomenon, and its instability is fundamental to the understanding of many MEMS devices [1,3]. The pull-in voltage can be used to determine the material properties, such as Young's modulus, plate modulus, and residual stress [6]. Accurate model on the pull-in voltage is helpful in designing electrostatic MEMS devices.

Most of previous works on pull-in voltage modeling were limited to straight shapes or forms free from residual stress [7–9]. However, residual deformations are very common in suspended micro structures, especially fabrication by surface micromachining process. Therefore, models to calculate pull-in voltage of cantilever beam subjected residual stress were also reported [10–13] by considering the curled deformation of the cantilever beams due to the gradient stress. Wei et al. [10] modified straight beam model to include curvature of beam. Hu investigated pull-in voltage calculation for curled cantilever beams by Euler–Bernoulli beam theory, Taylor's series expansion, and energy method [11]. The analytical models were further modified by considering fringing field effect [12] and the elastic boundary effect of the anchor point [13]. However, residual stress may include both gradient stress and mean stress. In that case, cantilever beam will deflect out-of-plane, with its far field curvature being generated exclusively by gradient stress and with an initial slope determined by both gradient stress and mean stress [14]. It means that the residual deformations of a suspended cantilever subject to both gradient stress and mean stress may have both curled and tilted deformations in general. Therefore, the corresponding pull-in voltage calculation should also consider both curled and tilted effects.

The purpose of this research aims to improve the pull-in voltage calculation by including both tilted and curled effects of suspended cantilevers in a modified deformation function. Cantilevers made of poly-silicon with different lengths at different locations will be fabricated and tested to examine the accuracy of the proposed model.

2. Model

For a flat micro cantilever beam with length L, width b, thickness h, and a Young modulus E, subjected to a downward electrostatic load, the pull-in voltage V_{PI} can be expressed as [9]:

$$V_{PI} = \sqrt{\frac{2h^3 G_0 E/(1-\nu^2)}{8.37\varepsilon L^4\left(\frac{5}{6G_0^2}+\frac{0.19}{G_0^{1.25}b^{0.75}}+\frac{0.19}{G_0^2 L^{0.75}}+\frac{0.4h^{0.5}}{G_0^{1.5}b}\right)}} \quad (1)$$

* Corresponding author. Tel.: +886 3 5712121 55111; fax: +886 3 5720634.
E-mail address: whsu@mail.nctu.edu.tw (W. Hsu).

0167-9317/$ - see front matter © 2014 Elsevier B.V. All rights reserved.
http://dx.doi.org/10.1016/j.mee.2013.12.030

where G_0, ε, and v are the initial air gap, permittivity of air, and Poisson's ratio, respectively. In Eq. (1), the beam is assumed to be initially straight with no axial tension/compression. However, the cantilever beam may have out-of-plane deformation after releasing the sacrificial layer in surface micromachining process, as shown in Fig. 1, therefore the predicted pull-in voltage by Eq. (2) could deviate significantly from the actual value. Since there is no constraint on the cantilever's free edge, the gradient component on the other hand provides a sensibly constant bending moment. As a result of such loading, the beam will curl as sketched in Fig. 1(b). Also, the boundary condition for anchor could involve zero displacement but a specified slope, as shown in Fig. 1(c), which is induced by the mean and gradient stresses in the original beam [14]. In short, under a general residual stress with gradient stress and mean stress, the cantilever beam may have out-of-plane curled and tilted deformations, with its far field curvature being generated exclusively by gradient stress and with an initial slope determined by both gradient and mean stress, as shown in Fig. 1(d).

To develop the analytical pull-in voltage solution of a cantilever beam with deformation, a mathematical function is needed to describe the deformation. For example, the curled deformation can be expressed as a function of the position x [10–13]:

$$G(x) = g_0 + \rho\left(1 - cos\frac{x}{\rho}\right) \tag{2}$$

where g_0 is the initial gap between the fixed end of the cantilever beam and the ground plane, and ρ is the radius curvature of the deformed beam. Here, a modified deformation function including both tilted and curled deformations on cantilever beam is proposed:

$$G(x) = g_0 + \rho\left(1 - cos\frac{x}{\rho}\right) + \theta \cdot x \tag{3}$$

where θ represents the tilted angle of the beam caused by gradient and mean stress.

The analytical pull-in voltage solution can be derived by energy method [15]. For a deformed cantilever beam subjected to a uniform electrical field, the total potential energy is the sum of the bending strain energy (U_m, based on the assumption of the Euler–Bernoulli beam) and the electrical potential energy U_e, i.e.

$$U = U_m + U_e = \frac{EI}{2}\int_0^L \left(\frac{d^2\omega}{dx^2}\right)^2 dx - \int_0^L \frac{\varepsilon b V^2}{2(G-\omega)}dx \tag{4}$$

where E, I, L, V, G, ω, ε, b, represent Young's modulus, the cross-sectional area moment of inertia, the beam length, the applied bias voltage, the initial gap between the beam and ground plane at position x, the deflection function at position x, the permittivity of air, and the beam width, respectively. Then, the deflection function $\omega(x)$ is assumed as:

$$\omega(x) = \eta\varphi(x) \tag{5}$$

where $\varphi(x)$ is the assumed deflection shape function satisfying the boundary conditions, and the coefficient η to be solved is the associated modal participation factor. At the transition from a stable to an unstable equilibrium state, the first-order and second-order derivatives of the total potential energy with respect to η both equal to zero, i.e.

$$\frac{\partial U}{\partial \eta} = EI\,\eta\int_0^L (\varphi'')^2 dx - \varepsilon b V^2 \int_0^L \frac{\varphi}{2(G-\eta\varphi)^2}dx = 0 \tag{6}$$

$$\frac{\partial^2 U}{\partial \eta^2} = EI\int_0^L (\varphi'')^2 dx - \varepsilon b V^2 \int_0^L \frac{\varphi^2}{(G-\eta\varphi)^3}dx = 0 \tag{7}$$

Solving Eq. (6) can determine η_{PI}, and then solving Eq. (7) can lead to the closed form of the pull-in voltage V_{PI} as:

$$V_{PI} = \sqrt{\frac{EI}{\varepsilon b}\times\frac{\int_0^L (\varphi'')^2 dx}{\int_0^L \frac{\varphi^2}{G^3}dx + 6\eta_{PI}\int_0^L \frac{\varphi^3}{G^4}dx + 12\eta_{PI}^2\int_0^L \frac{\varphi^4}{G^5}dx}} \tag{8}$$

By substituting the proposed modified deformation function $G(x)$, Eq. (3), into Eq. (8), the corresponding pull-in voltage solution considering both curled and tilted effects can be found. Similarly, substituting Eq. (2) into Eq. (8) can lead to the analytical pull-in voltage solution considering only curled effect for comparison. The integral terms in Eq. (8) are all constants related to the geometrical parameters of the beam, including ρ and θ in $G(x)$, which need to be identified experimentally. (The detailed solutions of $\varphi(x)$ and η_{PI} are listed in Supplementary data).

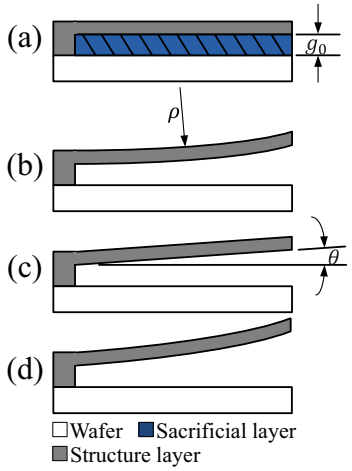

Fig. 1. States of a cantilever beam. (a) Initial state; (b) curled deformation; (c) tilted deformation; (d) deformation with both curled and tilted effects.

3. Experiments

3.1. Fabrication of cantilever beams

To examine the accuracy of the proposed model, cantilevers made of poly-silicon with different lengths at different locations are fabricated. The geometrical parameters and material properties of cantilever beams are listed in Table 1. Those beams are named as CB1, CB2, and CB3 for length 260, 295 and 330 μm, respectively.

The fabrication process of poly-silicon beams is illustrated in Fig. 2: (a) depositing gate oxide for CMOS circuit, (b) depositing the first poly-silicon layer and defining the wire and electrode, (c) depositing the isolation layer to avoid the electrical breakdown when pull-in happens, (d) depositing silicon oxide as sacrificial layer and defining the anchor of cantilever beam, (e) depositing second poly-silicon layer as structure layer, (f) releasing sacrificial layer to form suspended cantilever beam.

Table 1
The geometrical and material parameters of the cantilever beams.

Parameters	Descriptions	Values
L	Beam length	260/295/330 μm
b	Beam width	20 μm
h	Beam thickness	4.8 μm
g_0	Initial gap at fixed end	2 μm
L_a	Anchor length	2 μm
b_a	Anchor width	18 μm
h_a	Anchor thickness	4 μm
E	Young's modulus	160 GPa
ε	Permittivity of air	8.85×10^{-12} F/m

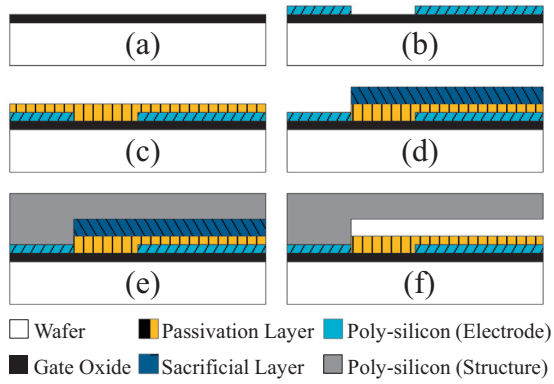

Fig. 2. Fabrication process of poly-silicon cantilever beam: (a) depositing gate oxide, (b) depositing the first poly-silicon layer, (c) depositing the isolation layer, (d) depositing silicon oxide, (e) depositing second poly-silicon layer, and (f) releasing sacrificial layer to form suspended cantilever beam.

3.2. Measurement setup for cantilever beam deformation and pull-in voltage

Deformation of cantilever beam can be measured by the white light interferometer (WLI) [16]. Here, we use Polytec MSA-500 Micro System Analyzer to acquire the cantilever beam geometry and radius of curvature (ρ). For measuring pull-in voltage, the cantilever beam is applied DC voltage on pads with probes, and then the beam is observed under WLI. The DC voltage will increase gradually until the free tip of the beam is sharply deflected downward. At that moment, the voltage is considered as the measured pull-in voltage. Other required instruments include a function generator (Agilent 33120A) to provide DC voltage from 0 to 5 V, and a power amplifier (A303 Piezo) to amplify the DC voltage up to twenty times.

4. Results and discussion

4.1. Fabrication results of cantilever beams

Fig. 3 shows the SEM pictures of fabricated cantilever beams: (a) length of CB1 is 259.66 μm, (b) length of CB2 is 295.30 μm, and (c) length of CB3 is 330.37 μm. The deviations between specification and fabricated results in beam length L are less than 0.1%, therefore 260/295/330 μm are used in Eq. (8) to calculate pull-in voltages. Similarly, fabricated beam thickness is found to range from 4.40 μm to 4.55 μm, therefore, the average 4.48 μm beam thickness is used in pull-in voltage calculations.

Here, two dies at different locations of the same 8-inch wafer are tested. One is located at the center of the wafer and the other one is at the wafer edge. Each die has three cantilever beams with three different lengths. Deformation profiles of all six cantilever beams are measured by WLI and shown in Fig. 4.

4.2. Radius curvature and tilted angle of cantilever beams

Based on the measured beam profile, WLI (Polytec MSA-500) can provide the best fitted radius of curvature of the beam. However, it is found that considering deformation all coming from curled effect, without tilted effect, can not describe the beam

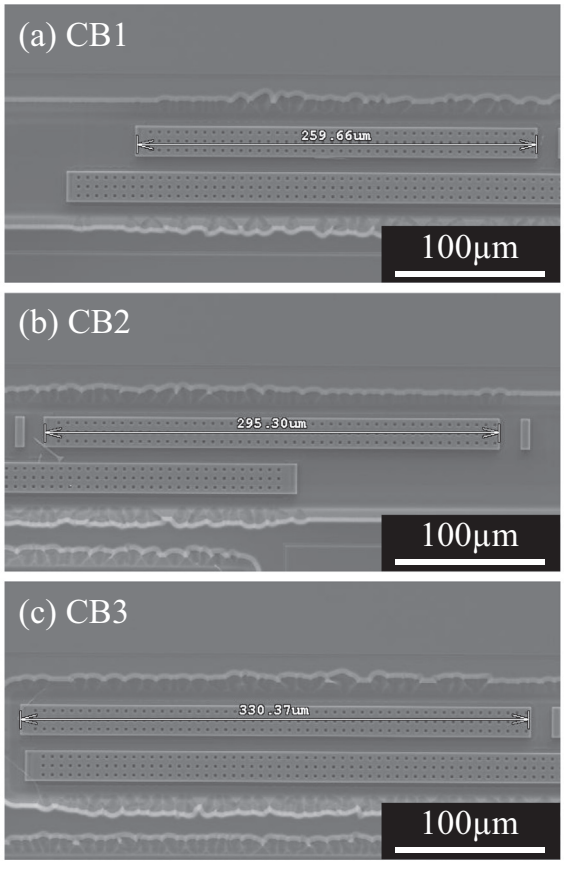

Fig. 3. SEM images of cantilever beams, (a) length of CB1 is 259.66 μm, (b) length of CB2 is 295.30 μm, and (c) length of CB3 is 330.37 μm.

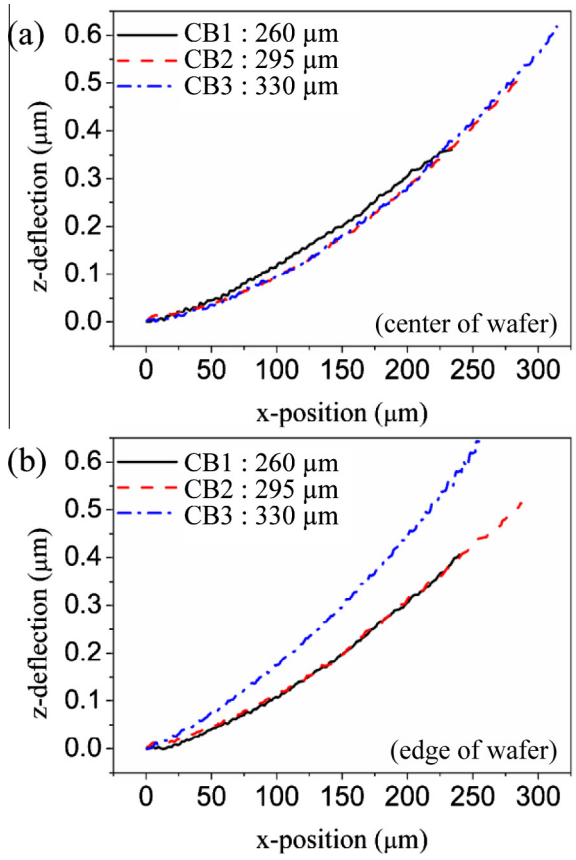

Fig. 4. Measured profiles of cantilever beams on two dies: (a) die at wafer center; (b) die near wafer edge.

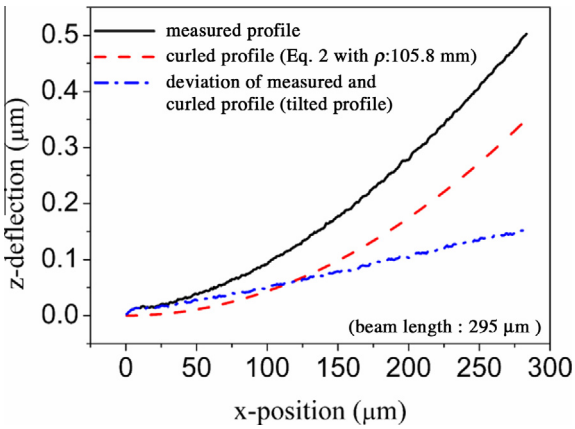

Fig. 5. Typical measured, curled, and tilted profiles of cantilever beam (beam length = 295 μm).

Table 2
The radius of curvature (ρ) and tilted angle (θ) of cantilever beams.

	Center of wafer			Edge of wafer		
	CB1	CB2	CB3	CB1	CB2	CB3
ρ (mm)	167.1	105.8	108.7	128.4	149.3	105.9
θ (10^{-3} rad)	0.61	0.53	0.65	0.56	0.55	1.30

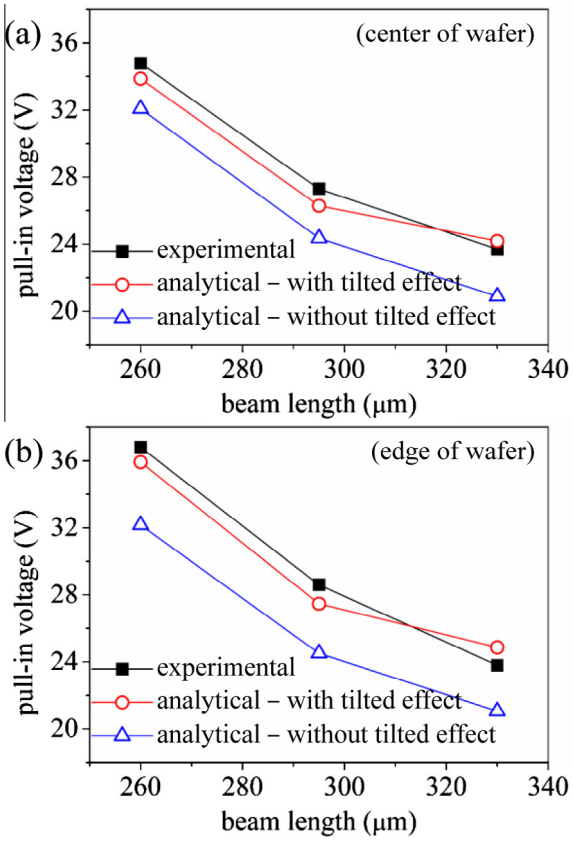

Fig. 6. Experimental and analytical results of pull-in voltages of cantilever beams at two dies: (a) die at wafer center; (b) die near wafer edge.

profile accurately. For example, from the measured profile of CB2 (solid line), as shown in Fig. 5, the calibrated radius of curvature, ρ, is found to be 105.8 mm. By using this calibrated radius of curvature, the corresponding curled profile calculated by Eq. (2) is plotted in Fig. 5 (dash line). There is evident difference between measured beam profile and calculated beam profile using calibrated radius of curvature. This deviation shown in Fig 5 (dash dot line) seems to be quite linear and is called tilted profile, since we consider this deviation coming from tilted effect. Then the tilted angle can be determined from this tilted profile. The radius of curvature of all six cantilever beams calibrated by WLI and the corresponding tilted angles are listed in Table 2. Once parameters ρ and θ are experimentally identified, the pull-in voltage can be calculated from the deformation function $G(x)$ and Eq. (8).

4.3. Pull-in voltages of cantilever beams

The calculated and measured pull-in voltages of cantilever beams at two dies are shown in Fig. 6. For analytical results without considering tilted effect, only curled effect, the average error is about 10.5%. For analytical results considering both curled and tilted effects, the average error is reduced to 3.2%, which verifies that modeling both curled and tilted effects in the proposed modified deformation function can effectively improve the accuracy of the pull-in voltage calculation.

5. Conclusion

This study proposes a modified deformation function which includes both tilted and curled deformations to improve the accuracy of the analytical solution of pull-in voltage. Poly-silicon beams with lengths of 260 μm, 295 μm and 330 μm are fabricated and tested to demonstrate the improvement of the proposed model. Radius of curvature ρ and tilted angle θ of deformed beams are experimentally identified from measured beam profiles. By comparing with measured pull-in voltages, it is shown that the average error of calculated pull-in voltages is reduced from 10.5% to 3.2% by considering tilted effect, which confirms the accuracy improvement of the proposed modified deformation function in pull-in voltage calculation.

Acknowledgments

This work was supported by the Grant number 101C090 of National Chiao Tung University. Nano Facility Center of National Chiao Tung University is also acknowledged for supporting fabrication and measurement facilities.

Appendix A. Supplementary data

Supplementary data associated with this article can be found, in the online version, at http://dx.doi.org/10.1016/j.mee.2013.12.030.

References

[1] H.A.C. Tilmans, R. Legtenberg, Sens. Actuator A-Phys. 45 (1994) 67–84.
[2] M. Maute, S. Raible, F.E. Prins, D.P. Kern, U. Weimar, W. Göpel, Microelectron. Eng. 46 (1999) 439–442.
[3] E.S. Hung, S.D. Senturia, J. Microelectromech. Syst. 8 (1999) 497–505.
[4] L. Jiang, M. Hassan, R. Cheung, A.J. Harris, J.S. Burdess, C.A. Zorman, M. Mehregany, Microelectron. Eng. 78–79 (2005) 106–111.
[5] P. Vettiger, J. Brugger, M. Despont, U. Drechsler, U. Dürig, W. Häberle, M. Lutwyche, H. Rothuizen, R. Stutz, R. Widmer, G. Binnig, Microelectron. Eng. 46 (1999) 11–17.
[6] P.M. Osterberg, S.D. Senturia, J. Microelectromech. Syst. 6 (1997) 107–118.
[7] S. Pamidighantam, R. Puers, K. Baert, H.A.C. Tilmans, J. Micromech. Microeng. 12 (2002) 458–464.

[8] Y.C. Hu, C.M. Chang, S.C. Huang, Sens. Actuator A-Phys. 112 (2004) 155–161.
[9] S. Chowdhury, M. Ahmadi, W.C. Miller, J. Micromech. Microeng. 15 (2005) 756–763.
[10] L.C. Wei, A.B. Mohammad, N.M. Kassim, Proc. ICSE (2002) 233–238.
[11] Y.C. Hu, J. Micromech. Microeng. 16 (2006) 648–655.
[12] Y.C. Hu, C.S. Wei, J. Micromech. Microeng. 17 (2007) 61–67.
[13] W.C. Chuang, Y.C. Hu, C.Y. Lee, W.P. Shih, P.Z. Chang, J. Micro-Nanolithogr. MEMS MOEMS 8 (2009) 033020.
[14] W. Fang, J.A. Wickert, J. Micromech. Microeng. 6 (1996) 301–309.
[15] I.H. Shames, C.L. Dym, Energy and Finite Element Methods in Structural Mechanics, McGraw-Hill, New York, 1985.
[16] C. O'Mahony, M. Hill, M. Brunet, R. Duane, A. Mathewson, Meas. Sci. Technol. 14 (2003) 1807–1814.